Numerical Study of the Implications of Size Nonuniformities in the Performance of Photonic Crystal Couplers Using Coupled Mode Theory

Thomas Kamalakis and Thomas Sphicopoulos

***Abstract*—Photonic crystals (PCs) are a promising technology for the realization of high-density optical integrated circuits. PC-based couplers have been proposed as a compact means of achieving wavelength multiplexing and demultiplexing. However, the performance of such devices can be limited by fabrication imperfections such as rod size nonuniformities. In this paper, coupled mode theory (CMT) is applied in order to study the implication of the variation of the size of the rods. CMT can provide a useful insight in the effect of size variations, and unlike other numerical methods such as the finite difference time domain, it does not require excessive computational time. Using CMT, the relation between the size nonuniformities and the coupler's insertion loss and extinction ratio is analyzed. It is shown that even a small size variation of the order of 2%–3% can degrade the performance of the device.**

***Index Terms*—Coupled mode analysis, couplers, photonic crystal, tolerance analysis, wavelength division multiplexing (WDM).**

I. Introduction

PHOTONIC crystals (PCs) [1], [2] are constantly attracting increased attention as a solution for the fabrication of ultracompact integrated optical circuits. The strong confinement of light in a PC waveguide, allows the realization of sharp waveguide bends, unlike the low index-contrast conventional optical integrated circuits in which the bending radii must be large (in order to limit bending losses). Large bending radii may increase the overall size of the integrated circuit [20]. The use of high index contrast waveguides [23] and PCs are expected to significantly decrease the size of optical integrated components. Various applications have been proposed that take advantage of the optical properties of PCs such ultracompact optical sources [3] and optical filters [4], [5]. The superprism effect may be used to realize small-size multiplexers/demultiplexers [6]. Nonlinear properties of PCs can also open a new possibilities such as the realization of compact all-optical transistors [7].

Optical couplers are important components of all-optical networks. PC-based optical couplers [8]–[12] consisting of two parallel PC waveguides have small beat lengths which reduces the overall size of the coupler. The small beat length is due to the fact that, in a PC coupler the refractive index contrast between the spheres or rods and the surrounding medium is high and hence, the difference between the effective index of the even and the odd mode can be quite large. This leads to very small beat lengths of the order of a few μm, allowing the exchange of optical power between the two PC waveguides over very short distances.

The performance of large PC-based devices is currently limited by the imperfections due to the fabrication process [13]. For example the size of the rods can vary by 2%–5% [14]. Hence, there is some deviation from the ideal PC structure, which causes coupling between the forward and the backward propagating modes and which in turn can increase optical losses due to reflections. Performance degradation can also be attributed to other factors such as the reflection from the waveguide bends (even in the absence of fabrication-induced structural deviations). However, these kind of reflection can be dealt, with a proper bend design [22]. Hence, fabrication tolerances can eventually set the limit in the performance of PC-based devices.

In this paper, the recently developed coupled mode theory (CMT) for periodic structures [15], [16] is applied in order to study the effect of random size variations of the rods due to fabrication imperfections in the performance of the PC coupler. Although the study of fabrication tolerances can, in principle, be accomplished by more powerful methods, like the finite difference time domain (FDTD) method [17], such methods are computationally expensive. In order to accurately study the fabrication tolerances, many sample devices, each having different structural deviations of the same variance σ^2 must be considered and the total number of samples that need to be numerically simulated may increase significantly. Hence, if computationally expensive techniques such as the FDTD are employed, then the total time required to calculate their response may increase impractically, making such numerical studies very difficult. On the other hand, CMT does not require a large amount of time to compute the response of each sample. CMT can also provide a useful physical insight in the effect of size nonuniformities. Within the CMT framework, the size nonuniformities directly perturb the coupling coefficients, creating coupling between the forward and the backward modes. The perturbation of the coupling coefficient between two modes is given as an integral of the perturbation $\Delta\varepsilon$ of the electric permittivity and the mode functions of the ideal structure. However, the basic drawback of the CMT is that it cannot handle devices with sharp waveguide bends.

The CMT can be used to study the impact of fabrication tolerances in conventional waveguides as well. For example in [18],

Manuscript received November 15, 2004; revised February 25, 2005. This work was supported in part by the PYTHAGORAS Grant of the Hellenic Ministry of Education.

The authors are with the Department of Informatics and Telecommunication, University of Athens, Athens GR15784, Greece (e-mail: thkam@di.uoa.gr; thomas@di.uoa.gr).

Digital Object Identifier 10.1109/JQE.2005.847543

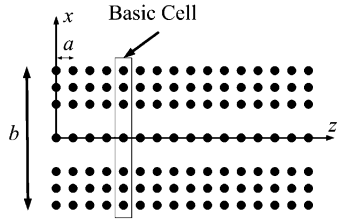

Fig. 1. Two-dimensional PC coupler formed by removing two rows of rods in a square lattice.

the authors have studied the effect of correlation of phase errors due to coupling in the grating arms of an Arrayed-Waveguide Grating (AWG) multiplexer.

The rest of the paper is as follows: In Section II, the wave propagation in ideal PC-based couplers is discussed. Issues concerning the mode normalization are emphasized. In Section III, the coupling between the modes due to structural deviations is discussed while in Section IV, the coupling coefficient perturbation due to rod size nonuniformities is calculated. In Section V, the numerical solution of the coupled mode equation is analyzed and in Section VI, the transfer function of a PC-based coupler is calculated. The results of these sections are then applied in Section VII, to estimate the expected power losses and extinction ratio degradation due to the size nonuniformities.

II. Wave Propagation in Ideal Couplers

A. Ideal Coupler Eigenmodes

Ideally, PC-based couplers are periodic structures along one direction, for example the z-direction, i.e., there exists a period a for which the dielectric constant ε obeys, $\varepsilon(x,y,z) = \varepsilon(x,y,z+a)$. An example of a 2-D PC coupler is shown in Fig. 1. The coupler is formed by removing two series of dielectric rods along the z-direction in a square lattice. In this case, the period a, is the center-to-center distance between two consecutive rods.

In order to apply the CMT in periodic structures such as PC-based couplers, it is useful to cast Maxwell's equations in the form of a generalized Hermitian eigensystem [19]. This is accomplished by expressing the electric and magnetic field components in one direction, say the z-direction, with respect to their transverse components $\mathbf{E}_t$, $\mathbf{H}_t$, respectively. Using Bloch's theorem, one may decompose the electromagnetic field of the periodic structure, into a set of Bloch waves of the form $(\mathbf{E}_t, \mathbf{H}_t)^T = |\beta\rangle e^{j\beta z}$ where $|\beta\rangle$ is a vector function, periodic function along z with period equal to a, satisfying the eigenproblem

$$\left(\widehat{A} + j\frac{\partial}{\partial z}\widehat{B}\right) \mid \beta\rangle = \beta\widehat{B} \mid \beta\rangle \tag{1}$$

where

$$\widehat{A} = \begin{pmatrix} \omega\varepsilon - \frac{1}{\omega}\nabla_t \times \frac{1}{\mu}\nabla_t \times & 0 \\ 0 & \omega\mu - \frac{1}{\omega}\nabla_t \times \frac{1}{\varepsilon}\nabla_t \times \end{pmatrix} \tag{2}$$

$$\widehat{B} = \begin{pmatrix} 0 & -\mathbf{z}\times \\ \mathbf{z}\times & 0 \end{pmatrix}. \tag{3}$$

In (2), ω is the angular wave frequency and μ is the magnetic permeability. The eigenfunctions $|\beta\rangle$ obey the following orthogonality relation

$$\langle \beta_1^* \mid \widehat{B} \mid \beta_2\rangle = \begin{cases} 0, & \beta_1 \neq \beta_2 \\ \eta_1, & \beta_1 = \beta_2 \end{cases} \tag{4}$$

where $\langle\psi_1|\psi_2\rangle$ is defined as

$$\langle \psi_1 \mid \psi_2\rangle = \int_A (\mathbf{E}_{t1}^* \cdot \mathbf{E}_{t2} + \mathbf{H}_{t1}^* \cdot \mathbf{H}_{t2})\, dA. \tag{5}$$

In (5), the asterisk denotes complex conjugation, $|\psi_i\rangle = (\mathbf{E}_{t_i}, \mathbf{H}_{t_i})^T$ with $i = 1, 2$ (the superscript T denotes transpose) and A is the surface [in two-dimensional (2-D) problems or volume [in three-dimensional (3-D) problems] of the basic unit cell. The basic unit cell for the 2-D coupler is shown in Fig. 1.

If both the discrete (guided) and the continuous (radiation) spectrum of eigenvalues are considered, then the functions $|\beta\rangle e^{j\beta z}$ form a complete set. Considering the guided modes of the structure only, the electromagnetic field may be written as a linear combination of the guided modes

$$\mid \psi\rangle = \sum_n C_n \exp(j\beta_n z) \mid \beta_n\rangle \tag{6}$$

where the sum includes both the forward ($\beta_n > 0$) and the backward propagating modes ($\beta_n < 0$) while C_n denotes the excitation coefficients mode n.

The eigenmodes $|\beta\rangle$ can be calculated using the well known plane-wave expansion technique. For example in the case of TM_y waves in 2-D structures (where $\partial/\partial y = 0$), it is relatively straightforward to show that the eigenproblem (1) is equivalent to a 2-D wave equation for the y-directed electric field component of $|\beta\rangle e^{j\beta z}$ designated by E_y. This equation can be easily solved expanding E_y as a series of plane waves

$$E_y(\mathbf{r}_2) = u_y(\mathbf{r}_2)e^{j\beta z} = \sum_G e(\mathbf{G}) \exp(j\mathbf{G}\cdot\mathbf{r}_2 + j\beta z) \tag{7}$$

where $e(\mathbf{G})$ are the plane-wave coefficients, $\mathbf{r}_2 = (x, 0, z)^T$, $\mathbf{G} = 2\pi(n/b, 0, m/a)$, m and n are integers and b the size of the basic cell along the x direction (as shown in Fig. 1). The full details of the plane wave expansion method can be found in [2].

As in conventional couplers, the spectral response of the PC-based coupler is due to the interference of the forward propagating modes. In a PC-based device, the two modes can have quite different propagation constants, implying a small beat length, which can be much smaller than that of a conventional coupler. In an ideal PC coupler, the two modes propagate uncoupled, i.e., no power transfer takes places between them, and no power is transferred to the backward propagating modes. As it will be shown in Section III, coupling between the modes can occur due to the existence of fabrication-induced nonuniformities.

B. Normalization of the Eigenmodes

Before CMT can be applied, the normalization of the eigenmodes of the structure must be considered. Since the modes are

calculated by the plane-wave expansion method, it is useful to express $\langle\beta^*|\widehat{B}|\beta\rangle = \eta_\beta$ in terms of the plane-wave coefficients $e(\mathbf{G})$. For the 2-D TM$_y$ modes, it can be shown that

$$\eta_\beta = \frac{2\beta}{\omega\mu_0}\int_A |u_y|^2 dA + \frac{2}{\omega\mu_0}\mathrm{Im}\left(\int_A u_y^* \frac{\partial u_y}{\partial z} dA\right). \quad (8)$$

The above result is deduced by expressing the magnetic field components in terms of E_y and using the fact that, according to Bloch's theorem, E_y can be written as $u_y(\mathbf{r}_2)e^{j\beta z}$ as in (7). In (8), A is the surface of the basic cell ($|x| \le b/2$ and $|z| \le a/2$). Expanding u_y in terms of plane waves as in (7), the following result can be obtained

$$\eta_\beta = \frac{2}{\omega\mu_0} A \sum_G |e(\mathbf{G})|^2 (\beta + G_z) \quad (9)$$

where G_z is the z component of $\mathbf{G}$. To derive (9), one uses the fact that the functions $\exp(j\mathbf{G}\mathbf{r})$ obey the property

$$\int_A \exp(j(\mathbf{G}-\mathbf{G}')\cdot\mathbf{r}_2)dA = \begin{cases} 0, & \mathbf{G} \neq \mathbf{G}' \\ A, & \mathbf{G} = \mathbf{G}'. \end{cases} \quad (10)$$

It is interesting to note that the direction of the mode, influences the value of (10). Indeed, let $\beta > 0$ correspond to a forward propagating mode and let u_β be its Bloch function. Then by the symmetry of the eigenproblem [2], one can show that there exists a backward propagating mode whose propagation constant is $-\beta$ and its Bloch function $u_{-\beta}$, is the complex conjugate of u_β, i.e.,

$$u_{-\beta} = u_\beta^*. \quad (11)$$

Hence, the E_y component of the backward mode is

$$E_y(\mathbf{r}) = u_y^*(\mathbf{r})e^{-j\beta z} = \sum_G e^*(\mathbf{G})\exp(-j\mathbf{G}\cdot\mathbf{r} - j\beta z). \quad (12)$$

Equation (12) suggests that the value of $\eta_{-\beta}$ can be obtained from (12) by replacing $\mathbf{G}$ with $-\mathbf{G}$ and $e(\mathbf{G})$ with $e^*(\mathbf{G})$ in (12). The result is

$$\eta_{-\beta} = -\frac{2}{\omega\mu_0} A \sum_G |e(\mathbf{G})|^2 (\beta + G_z) = -\eta_\beta. \quad (13)$$

The forward propagating modes can be normalized, so that $\eta_\beta = (2/\omega\mu_0)$. To satisfy (13), the backward propagating modes are normalized so that $\eta_{-\beta} = -(2/\omega\mu_0)$. This distinction between the normalization of the forward and backward modes is important, in order to accurately apply the CMT in Sections III–VII.

III. Coupling Due to Size Non-Uniformities

The electromagnetic field expansion given by (8) is valid for the ideal PC coupler. Size nonuniformities change the value of the electric permittivity by a small amount $\Delta\varepsilon$. In this case the operator equation of (1) is written as [16]

$$\widehat{A} \mid \psi\rangle + \Delta\widehat{A} \mid \psi\rangle = -j\frac{\partial}{\partial z}\widehat{B} \mid \psi\rangle \quad (14)$$

where

$$\Delta\widehat{A} = \begin{pmatrix} \omega\Delta\varepsilon & 0 \\ 0 & \frac{-1}{\omega}\nabla_t \times \Delta\left(\frac{1}{\varepsilon}\right)\nabla_t \times \end{pmatrix} \quad (15)$$

is considered a small perturbation. The electromagnetic field is now written as

$$\mid \psi\rangle = \sum_n C_n(z)\exp(j\beta_n z) \mid \beta_n\rangle \quad (16)$$

i.e., the excitation coefficients $C_n(z)$ of the backward and forward propagating modes are now z-dependent. To determine $C_n(z)$, one could think of applying the procedure used in conventional (constant cross-section) waveguides. Namely, (16) can be substituted in (14) and the orthogonality relations of the modes can be used to determine the z-dependence of $C_n(z)$. In conventional waveguides, the domain of integration A is a surface or a line transverse to z and the modal fields $|\beta_n\rangle$ are z-independent. This allows the derivation of a system of coupled equations describing the evolution of $C_n(z)$ by applying the orthogonality relations [21]. In periodic structures, however, the problem with this approach is that the domain of integration A is the entire unit cell and hence involve integration along the z-direction as well. The modal fields $|\beta_n\rangle$ also depend on z. Therefore, the orthogonality relations can not be applied directly to derive a system of coupled equations describing the evolution of $C_n(z)$ since the variable z can not be separated. This problem was addressed recently in [16], by introducing a change of variable $z \rightarrow z + z_1$, z_1 being a fictitious displacement of the original periodic structure, in (16) and (14). The orthogonality relations are then applied by performing the integration along z_1 and not z, permitting the derivation of the following system of coupled equations [16]

$$\frac{dc_{mk}}{dz} = \sum_{nl} A_{mknl}c_{nl} \quad (17)$$

where the original excitation coefficient C_m for mode m is related to c_{mk} through

$$C_m(z) = \sum_k c_{mk}(z) \quad (18)$$

where k takes integer values. The coupling coefficients A_{mknl} are related to the perturbation by

$$A_{mknl} = e^{j(\beta_n - \beta_m)z} \times \left\langle \beta_m^*(z+z_1) \mid \Delta\widehat{A}e^{-j2\pi(l-k)/a} \mid \beta_n(z+z_1)\right\rangle. \quad (19)$$

The integration in $\langle , \rangle$ is now along z_1 instead of z. Using a change of variable, A_{mknl} for a 2-D system is written as:

$$A_{mknl} = j\eta_m\omega e^{j(\beta_n - \beta_m + 2\pi(l-k)/a)z} \times \int_A dx'dz'\Delta\varepsilon(x',z)u_y^{m^*}(x',y')u_y^n(x',y') \times e^{-j2\pi(l-k)z'/a}. \quad (20)$$

The system of coupled differential equations can be used to find the solution of the excitation coefficients $C_n(z)$ [16]. Equation (20) relates the perturbation $\Delta\varepsilon$ to the coupling coefficients

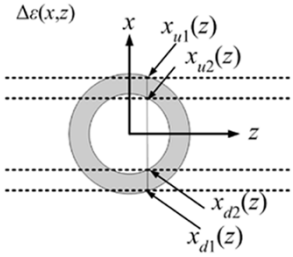

Fig. 2. Perturbation $\Delta\varepsilon$ obtained by changing the radius of a single rod.

of the modes. The effect of the perturbation is more clearly seen by transforming the coupling coefficients as

$$\overline{c}_{mk} = e^{j(\beta_m + 2\pi k/a)z} c_{mk} \tag{21}$$

in which case the new excitation coefficients are given by

$$\frac{d\overline{c}_{mk}}{dz} = \sum_{nl} (B^0_{mknl} + \Delta B_{mknl})\overline{c}_{nl} = \sum_{nl} B_{mknl}\overline{c}_{nl} \tag{22}$$

and

$$B^0_{mknl} = j\eta_m \omega \delta_{mn}\delta_{kl} \tag{23}$$

$$\Delta B_{mknl} = j\eta_m \omega \int_A dx'dz' \Delta\varepsilon(x',z) u_y^{m^*}(x',y') u_y^n(x',y') \times e^{-j2\pi(l-k)z'/a}. \tag{24}$$

In the absence of perturbations, the differential equations (22) are uncoupled since $\Delta B_{mknl} = 0$. The perturbation $\Delta\varepsilon$ causes the equations to become coupled. Note that the amount of coupling depends on the strength of the perturbation and on the strength of the modal profiles on the pertubation.

IV. Calculation of the Coupling Coefficients

Equation (24) can be used to estimate the value of the coupling coefficients of the PC coupler modes. The integral of (24) can be computed by numerical techniques once the modal fields u_y^n and the perturbation $\Delta\varepsilon$ are determined. The modal fields can be computed through the plane-wave expansion method. To determine $\Delta\varepsilon$, we consider changing the radius of a single rod from r to $r + \Delta r$ as shown in Fig. 2.

The grey shaded surface in Fig. 2 is the region C of the (x, z) plane for which $\Delta\varepsilon$ is nonzero. If Δr is positive, then the values of (x, z) inside C obey $r^2 \le x^2+z^2 \le (r+\Delta r)^2$ and the value of $\Delta\varepsilon$ in this region is $g = \varepsilon_0(n_r^2-1)$, where n_r is the refractive index of the rods (which are assumed to be surrounded by air). For $|z_0| \le r$, C intersects $z = z_0$ at four points, designated as $x_{u1}, x_{u2}, x_{d1}, x_{d2}$ in Fig. 2. It is easy to deduce that those four points are given by

$$\begin{aligned} x_{u1} &= r_1\sqrt{\frac{1-z^2}{r_1^2}} \\ x_{u2} &= r\sqrt{\frac{1-z^2}{r^2}} \\ x_{d1} &= -r_1\sqrt{\frac{1-z^2}{r_1^2}} \\ x_{d2} &= -r\sqrt{\frac{1-z^2}{r^2}} \end{aligned} \tag{25}$$

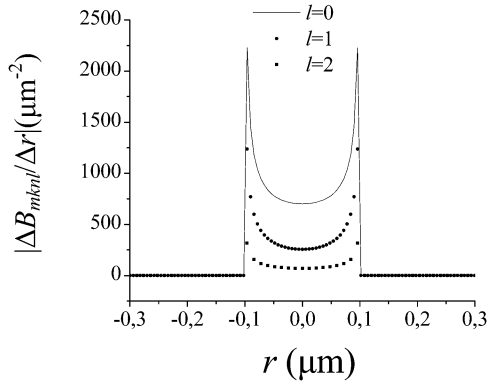

Fig. 3. Rate of change of the coupling coefficient ΔB_{mknl} for $m = 1, n = 1$, $k = 0$ and $l = 0, 1, 2$. The value of Δr is 0.1 nm.

with $r_1 = r + \Delta r$. Hence, the integral in (27) is written as

$$\begin{aligned} & g\int_{x_{u2}}^{x_{u1}} dx' \int_{-a/2}^{a/2} dz' u_y^{m^*}(x',y') u_y^n(x',y') \\ & \quad \times e^{-j2\pi(l-k)z'/a} \\ & + g\int_{x_{d2}}^{x_{d1}} dx' \int_{-a/2}^{a/2} dz' u_y^{m^*}(x',y') u_y^n(x',y') \\ & \quad \times e^{-j2\pi(l-k)z'/a}. \end{aligned} \tag{26}$$

A similar expression can be derived if $\Delta r < 0$ except that the position of x_{u1} and x_{d1} is now exchanged with x_{u2} and x_{d2}, respectively. Also, $g = \varepsilon_0(1 - n_r^2)$ for $\Delta r < 0$. Using the above relations, one can calculate $B_{mknl}(z)$ for $|z| \le r$. Similar considerations may be applied to evaluate $B_{mknl}(z)$ for $|z-r| \le |\Delta r|$. The integrals in (26) can be estimated by numerical integration techniques. It is also useful to note that as k and l vary, $B_{mknl}(z)$ depends only on k-l and not the actual values of k and l. In Fig. 3, the rate of change of the coupling coefficient $\Delta B_{mknl}/\Delta r$ of the forward propagating modes $(m = 1)$ and $(n = 2)$ is plotted for $k = 0$ and $l = 0,1,2$. It is deduced from Fig. 3, that the amplitude of the coupling coefficients quickly diminishes as $|l$-$k|$ increases and only few values of l around k can be considered. Indeed, for $|l$-$k| > 2$ the values of $\Delta B_{mknl}/\Delta r$ are negligible.

V. Solution of the CMT Equations

The system of differential (22) must be solved in order to estimate the change in the excitation coefficients of the eigenmodes and estimate the impact of fabrication imperfections in the performance of the PC-based coupler. Before solving the system it is more convenient to write (22) in vector form as

$$\frac{d\mathbf{c}}{dz} = E\mathbf{c} \tag{27}$$

where the components of the vector $\mathbf{c} = (c_i)^T$ are defined as

$$c_{Mm+k} = \overline{c}_{mk}. \tag{28}$$

In (28) M is the number of the guided modes considered. The elements of matrix $E = [E_{\text{ih}}]$ are given by

$$E_{Mm+k,Mn+l} = B_{mknl}. \tag{29}$$

A trial solution of (27) is

$$\mathbf{c}(z) = F(z)\mathbf{f} \tag{30}$$

with

$$F(z) = \exp\left(\int_0^z E(z')dz'\right) \tag{31}$$

and $\mathbf{f}$ a constant vector whose value must be determined in order to much the initial conditions of the problem. Note that although $E(z)$ and $E(z')$ may not in generally commute, (30) gives a very accurate estimate of the solution because the perturbation-induced z values of E were very small in all cases examined. At the device input, the forward modes are initially excited with amplitudes C_1^0 and C_2^0 and hence for the forward modes ($m = 1, 2$) one has $c_{10}(0) = C_1^0$, $c_{20}(0) = C_2^0$ and $c_{mk}(0) = 0$ for $k \neq 0$. It is also assumed that no reflection exists at the end of the device and hence $c_{mk}(Na) = 0$ if m refers to a backward propagating mode ($m = 3, 4$), where N is the length of the device along the z-direction measured in rods. Using (30) it can be easily shown that in order to satisfy these conditions, the following system of equations must hold for $\mathbf{f} = [f_k]$:

$$\sum_k F_{ik}(z_i) f_k = c_i(z_i) = d_i \tag{32}$$

where z_i equals 0 or Na depending on whether c_i refers to a forward or a backward propagating mode, respectively. Defining the matrix $\Omega = [\Omega_{pq}]$ to have elements $\Omega_{pq} = F_{pq}(z_p)$, the value of $\mathbf{f}$ the can be estimated from (32), using

$$\mathbf{f} = \Omega^{-1}\mathbf{d} \tag{33}$$

where $\mathbf{d}$ is the vector $[d_i]^T$. Equations (30), (31), and (34) can be used to solve the system of differential (22). The integral $\int E(z)dz = \left[\int E_{pq}(z)dz\right]$ of matrix $E(z)$ within a single cell in (31), can be estimated by calculating $\int E_{pq}(z)dz$ numerically. The matrix $F(z)$ is then estimated using the series expansion of the exponential of a square matrix S

$$\exp(S) = \sum_{n=0}^{\infty} \frac{S^n}{n!}. \tag{34}$$

The exponential of a matrix can be easily calculated in MATLAB.

Note that using this matrix to solve the system (27), one can also relate the amplitudes $C_n(z)$ of the forward and backward propagating modes at the coupler output, $z = Na$ to the amplitudes at $z = 0$

$$\mathbf{C}(Na) = F_C(Na)\mathbf{C}(0) \tag{35}$$

where the matrix $F_C(Na)$ can be formed using (30) and adding the relative Fourier components $c_{mk}(z)$ of each coupling coefficient $C_m(z)$ using (18). In this paper, the amplitude of the backward propagating mode at the coupler output is assumed zero. Hence, the CMT does not take into account reflections that can occur at the coupler output. However, in practical applications, the coupler output ports will be adjacent to another dielectric structure B (see Fig. 4) and there can be reflections at the interface due to modal mismatch. Such reflections can also occur at the coupler input where the coupler is adjacent to a dielectric structure A. If the modes of A and B are known, the excitation

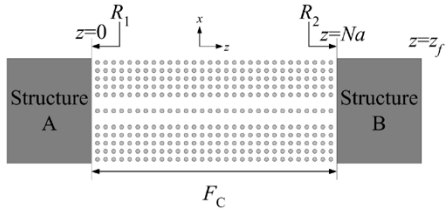

Fig. 4. PC coupler with two dielectric structure in its input and output ports.

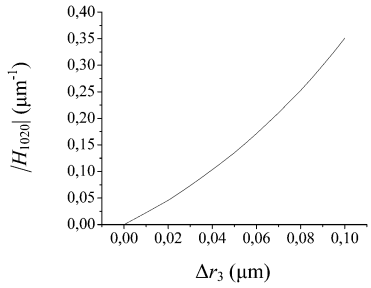

Fig. 5. Variation of $|H_{1020}|$ with respect to the variation of the radius of the third rod of the supercell of Fig. 1.

coefficients of the coupler Bloch modes can be calculated as in [25]. Applying the CMT will then yield

$$\mathbf{C}_B = R_1 F_C(Na) R_2 \mathbf{C}_A \tag{36}$$

where $\mathbf{C}_B$ and $\mathbf{C}_A$ are the modal amplitudes inside A and B, respectively at the interface with the coupler, R_1 is the matrix that converts the amplitudes of the modes of A to the amplitudes of the modes of the coupler and R_2 is the matrix that converts the amplitudes of the modes of the coupler to the amplitudes of the modes of B. Matrices R_1 and R_2 can be computed as in [25]. Assuming that there are no backward modes in structure B and only forward modes in structure A, one can use (36) in order to obtain the amplitudes of the modes at the input and the output of the coupler. The reflections encountered at the input and the output ports of the coupler are incorporated through the matrices R_1 and R_2.

It is useful to note that $H_{mknl} = \int \Delta B_{mknl}(z)dz$ within a single cell, exhibits a quasi-linear dependence on the variation Δr_p of the pth rod radius. As an example, the variation of H_{1020} with respect to Δr_3 is plotted in Fig. 5 for the PC based coupler of Fig. 1. It is evident that H_{1020} exhibits an almost linear behavior even for values of Δr_3 of the order of few nm. Hence, one may use the Taylor' series expansion to first order, to write

$$H_{mknl} \cong \sum_p \Delta r_p \left.\frac{\partial(H_{mknl})}{\partial(\Delta r_p)}\right|_{\Delta r_p = 0} = \sum_p \Delta r_p \alpha_{mknl}^{(p)} \tag{37a}$$

where

$$a_{mknl}^{(p)} = \left.\frac{\partial(H_{mknl})}{\partial(\Delta r_p)}\right|_{\Delta r_p = 0}. \tag{37b}$$

The coupler consists of many basic cells. Let Δr_{pq} denote the variation of the pth rod of the qth cell. Then the H_{mknl} is given by

$$H_{mknl} \cong \sum_{pq} \alpha_{mknl}^{(p)} \Delta r_{pq}. \tag{38}$$

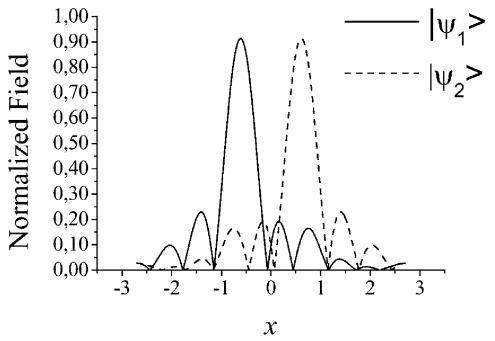

Fig. 6. Fields $|\psi_i\rangle$ for the coupler of Fig. 1 at the edge of the unit cell.

The coefficient $\alpha^{(p)}_{mknl}$ can be calculated by numerically estimating the derivatives of H_{mknl} with respect to Δr_p. Calculation of the H_{mknl} using (38) has the advantage that the derivatives $\alpha^{(p)}_{mknl}$ need to be computed only once for each ideal coupler design. Once the various $\alpha^{(p)}_{mknl}$ are computed, then the H_{mknl} can be estimated using (38) for many different values of the random variables Δr_{pq}. This allows the statistical study of many sample devices without excessive computational time requirements.

VI. Calculation of the Coupler Transfer Function

Given the excitation coefficients of the modes, the coupler power transfer function $T(\lambda)$ can be calculated. The values of $T(\lambda)$ can be used to quantify the effects of size nonuniformities on the performance of the device. To relate $T(\lambda)$ with the coupling coefficients, one considers the forward propagating field at the coupler output which is written as

$$|\,\psi\rangle = \overline{C}_1(Na)\,|\,\beta_1\rangle + \overline{C}_2(Na)\,|\,\beta_2\rangle \tag{39}$$

where $\beta_1 > 0$ and $\beta_2 > 0$ are the propagation constants of the even and odd forward propagating mode, respectively, and $\overline{C}_n = C_n e^{j\beta_n z}$. To find the transfer function of the output ports, the field of (39) is projected to the basis

$$|\,\psi_1\rangle = \frac{1}{\sqrt{2}}\,|\,\beta_1\rangle + \frac{j}{\sqrt{2}}\,|\,\beta_2\rangle \tag{40a}$$

$$|\,\psi_2\rangle = \frac{1}{\sqrt{2}}\,|\,\beta_1\rangle - \frac{j}{\sqrt{2}}\,|\,\beta_2\rangle. \tag{40b}$$

Due to the nature of the modes, the field $|\psi_1\rangle$ is mainly on the one output port, while $|\psi_2\rangle$ is on the other port. This is shown on Fig. 6, where the fields $|\psi_i\rangle$ are plotted at the edge of a unit cell. As seen by the figure $|\psi_1\rangle$ is mainly inside one of the waveguides and $|\psi_2\rangle$ is mainly on the opposite one. The normalized power transfer function for the second output port is $T_1(\lambda)$ is proportional to $|\langle\psi_1|\mathbf{B}|\psi\rangle|^2$ and equals

$$T_1(\lambda) = \frac{|\overline{C}_1(Na) + j\overline{C}_2(Na)|^2}{2}. \tag{41}$$

Assuming that the incident field is equal to $|\psi_2\rangle$ (i.e., that the optical power at the input is located on the other PC waveguide), one obtains from (40) the initial conditions $c_{10}(0) = 1/\sqrt{2}$ and $c_{20}(0) = -j/\sqrt{2}$. In the absence of size nonuniformities, it is easy to deduce from (22) that the coupling coefficients evolve as

$$\overline{c}_{mk}(z) = c_{mk}(0)e^{j\beta_m z + j2\pi k z/a}. \tag{42}$$

In this case, $T_1(\lambda)$ becomes

$$T_1(\lambda) = \frac{|1 + \cos((\beta_1 - \beta_2)\,Na)|^2}{4}. \tag{43}$$

Equation (43) is the power transfer function of the ideal PC coupler without any size nonuniformities and is similar to the power transfer function of a conventional coupler.

In order to estimate the accuracy of the CMT, it is interesting to compare (43) with the results of FDTD. In order to accomplish this, the 2-D geometry of Fig. 7(a) is considered. A single mode PC waveguide is adjacent to an input port of a PC coupler formed by two single mode waveguides separated by a single row of rods. The coupler length is $N = 20$ rods, the rod radius is $r = 0.1$ μm and the rod spacing is $a = 0.6$ μm. To prevent reflections due to the finite computational area, the perfectly matched layer (PML) boundary conditions are employed [26]. The shaded regions in Fig. 7(a) correspond to the PML layers. The fundamental mode of the single mode waveguide is excited using the total field/reflected field formulation [17] with a Gaussian pulse having a $1/e$ intensity point equal of 10 fs. As time elapses, the values of the electric field are recorded at the coupler input and output ports. The transfer function of the coupler is estimated from the ratio of the spectra of the fields measured at the output ports and the field measured at the input

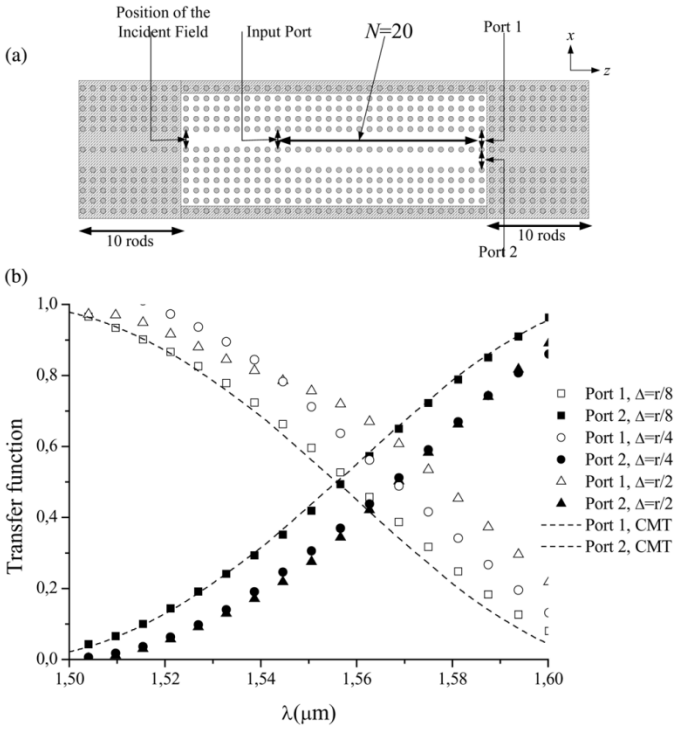

Fig. 7. (a) Geometry used for comparison of FDTD and CMT. (b) Transfer function for the output ports of the coupler obtained by FDTD and CMT.

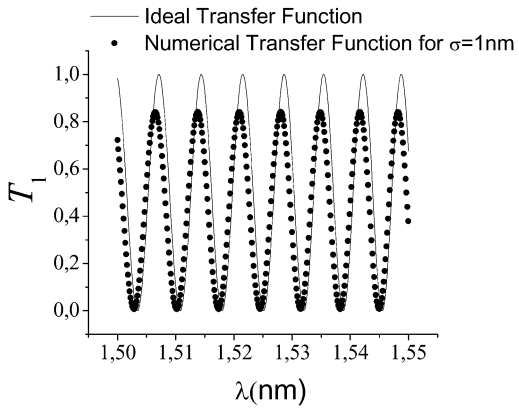

Fig. 8. Transfer function of the ideal and the nonuniform PC coupler.

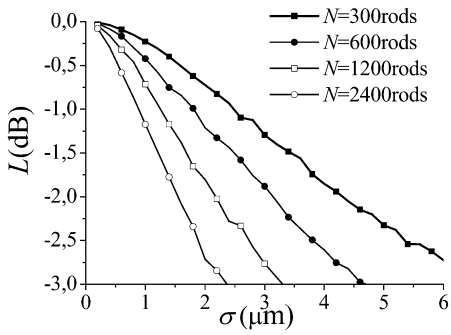

Fig. 9. Mean value (in decibels) of the loss L due to coupling with the backward propagating modes for various values of σ for various coupler lengths N.

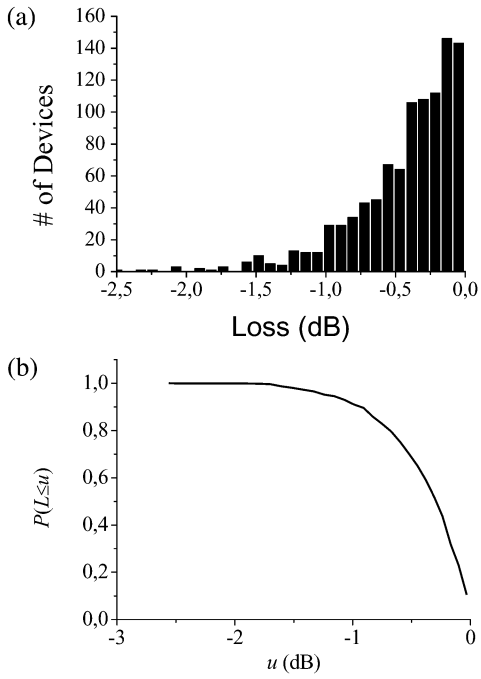

Fig. 10. (a) Histogram of the loss values of the numerically calculated devices for $\sigma = 1$ nm and $N = 600$. (b) cumulative probability density function of the loss L.

port. In Fig. 7(b) the coupler transfer function obtained for various FDTD grid steps Δ are plotted along with the transfer function obtained by the CMT. As the grid becomes finer and Δ is reduced, the results of the FDTD method converge to those obtained by the CMT. For $\Delta = r/8$, the agreement is very good, and this is a strong indication of the validity of the CMT. In [12], a comparison between the CMT and the finite element time domain beam propagation method (FETD-BPM) was also carried out assuming coupler geometries with sharp bend at the output ports. Although, as mentioned in the introduction, reflections from the bends cannot be incorporated the CMT, the CMT still gave a reasonable estimate for the transfer function of the devices.

VII. Results and Discussion

The CMT outlined in the preceding sections will now be applied to analyze the performance degradation of PC-based couplers due to size nonuniformities. In Fig. 8, the power transfer function of the ideal PC coupler is plotted with solid lines along with the transfer function of a PC coupler whose rods radii vary randomly. The perturbations of the radii of the rods are chosen so that their mean value is zero, using a Gaussian random generator with standard deviation $E\{\Delta r_{pq}^2\}^{1/2} = \sigma = 1$ nm. Both couplers have length $N = 600$ rods. By comparing the peaks of the two transfer functions, it is evident that there is about 1-dB insertion loss in the case of the nonideal coupler. This insertion loss is due to the power reflected at the device input due to the coupling of the backward with the forward propagating modes. There is also some wavelength shift of the transfer function of the perturbed device.

To further analyze the optical losses due to reflection, various values of σ are considered. For each value of σ, 1000 sample devices are used to numerically estimate the mean power loss. The results are plotted in Fig. 9, in the case of N =300, 600, 1200, and 2400 rods. It is evident that the losses can be quite significant especially for values of $\sigma > 2$ nm for the long devices. For example, in the case where $\sigma = 2$ nm, the average losses are about -1 dB and -2.5 dB for N =600 and 2400, respectively. This means that size nonuniformity can pose important limitations in PC devices due to the power coupled to the backward propagating modes. For $\sigma = 2$ nm, the relative size change is $\sigma/r = 2\,\text{nm}/100\,\text{nm} = 2\%$, which is a relatively small value even for state-of-the-art fabrication techniques. It is also interesting to note that in order to achieve power loss less than 0.5 dB, σ should be smaller than 1 nm in the case of $N = 2400$, implying a relative size change σ/r of the order of 1%. Hence, to achieve ultralow-loss PC based couplers, the size nonuniformities must be limited to less than 1%.

In Fig. 10(a), the histogram of the loss values of the numerically calculated devices is plotted for $\sigma = 1$ nm and $N = 600$. It is deduced that the majority of the devices have loss values smaller than the average loss which in this case is -0.4 dB. In most of the devices the loss does not exceed -1.0 dB but there are few, whose loss is higher than -1.0 dB. This behavior is not surprising since the rods that are nearer to the PC waveguide core are expected to have the strongest influence. If the largest deviations are located near the waveguide cores, the device may have significantly higher losses than the devices where the rods with large deviations are found both near and far from the cores

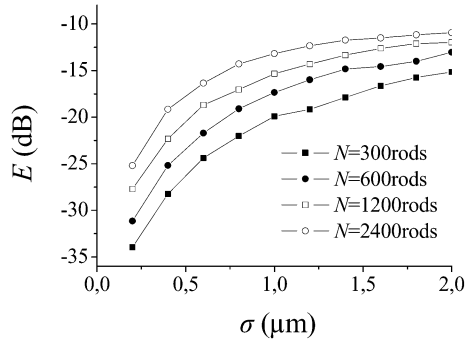

Fig. 11. Mean value (in decibels) of the extinction ration E due to size nonuniformities for various values of σ.

(which constitutes the most likely case). In Fig. 10(b), the cumulative distribution function (CDF) $P(L \leq u)$ of the loss L is also plotted.

Note that conventional (nonPC based) devices like fiber Bragg gratings can have very low insertion losses, even less than -1 dB. From Fig. 10(b) it is deduced that about 90% of the devices had insertion losses less than -1 dB. This implies $\sigma = 1$ nm guarantees that about 90% of the fabricated 600-rod couplers will be expected to have low insertion loss (less than -1 dB).

Another important parameter which characterizes the coupler performance is its extinction ratio which is defined as the ratio of the higher and the lowest value of $T(\lambda)$. Ideally the coupler should have large extinction ratio, especially if it is used for filtering applications. In Fig. 11, the mean extinction ratio E of a PC-based coupler is plotted for various values of σ. It is deduced that the extinction ratio may be degraded even for small σ. For example in the case of $\sigma = 1$ nm, the average extinction ratio rises to -20 dB for $N = 600$ and -13 dB for $N = 2400$. If the coupler is used as a filter for WDM applications, this suggests that the crosstalk noise from the other channels may become a problem, necessitating the use of additional filtering at the receiver. Hence, the need for low channel crosstalk also underlines the need for high quality fabrication methods with low size nonuniformities.

The above results indicate that size nonuniformities can severely degrade the performance of large PC-based components such as long couplers. It should however be pointed out that for many novel PC applications the device size is smaller and therefore the influence of fabrication tolerances is much less important as discussed in [24].

VIII. Conclusions

In this paper, CMT for periodic structures has been applied to analyze the effect of size nonuniformities in a PC-based coupler. Unlike other numerical methods (like FDTD), CMT does not require an excessive amount of time to calculate the spectral response of a large number of sample devices. It also provides a physical insight on the way in which the size nonuniformities influence the performance of the device. Using CMT, it was numerically shown that in long PC couplers, even small size nonuniformities can cause significant loss values due to the coupling between the forward and backward propagating modes. This can pause stringent requirements on the fabrication of such devices, if the device size is large. The size nonuniformities have also been shown to increase the extinction ratio of the coupler, degrading its filtering characteristics and probably necessitating the use of additional filtering at the receiver to avoid crosstalk noise from signals at other wavelengths.

References

[1] J. D. Joannopoulos, R. D. Meade, and J. N. Winn, *Photonic Crystals, Molding the Flow of Light*. Princeton, NJ: Princeton Univ. Press, 1995.
[2] K. Sakoda, *Optical Properties of Photonic Crystals*. Berlin, Germany: Springer-Verlag, 2001.
[3] I. Vurgaftman and J. R. Meyer, "Photonic-Crystal distributed-feedback quantum cascade lasers," *IEEE J. Quantum Electron.*, vol. 38, no. 6, pp. 592–602, Jun. 2002.
[4] M. Imada, S. Noda, A. Chutinan, M. Mochizuki, and T. Tanaka, "Channel drop filter using a single defect in a 2-D photonic crystal slab waveguide," *J. Lightw. Technol.*, vol. 20, no. 5, pp. 873–878, May 2002.
[5] R. Costa, A. Melloni, and M. Martinelli, "Bandpass resonant filters in photonic-crystal waveguides," *IEEE Photon. Technol. Lett.*, vol. 15, no. 3, pp. 401–403, Mar. 2003.
[6] T. Matsumoto and T. Baba, "Photonic crystal k-Vector superprism," *J. Lightw. Technol.*, vol. 22, no. 3, pp. 917–922, Mar. 2004.
[7] M. F. Yanik, S. Fan, M. Soljačić, and J. D. Joannopoulos, "All-optical transistor action with bistable switching in a photonic crystal cross-waveguide geometry," *OSA Opt. Lett.*, vol. 28, no. 24, pp. 2506–2508, Dec. 2003.
[8] M. Thorhauge, L. H. Frandsen, and P. I. Borel, "Efficient photonic crystal directional couplers," *OSA Opt. Lett.*, vol. 28, no. 17, pp. 1525–1528, Sep. 2003.
[9] I. Park, H. S. Lee, H. Kim, K. Moon, S. Lee, B. Hoan, S. Park, and E. Lee, "Photonic crystal power-splitter based on directional coupling," *Opt. Exp.*, vol. 12, no. 15, pp. 3599–3604, Jul. 2004.
[10] M. Thornhauge *et al.*, "Properties of directional couplers using photonic crystal waveguides," in *Proc. OFC*, 2003, pp. 494–494.
[11] C. Y. Liu and L. W. Chen, "Tunable photonic crystal waveguide coupler with nematic liquid crystals," *IEEE Photon. Technol. Lett.*, vol. 16, no. 8, pp. 1849–1851, Aug. 2004.
[12] M. Koshiba, "Wavelength Division Multiplexing and Demultiplexing With Photonic Crystal Waveguide Couplers," *J. Lightw. Technol.*, vol. 19, no. 12, pp. 1970–1975, Dec. 2001.
[13] H. Y. Ryu, J. K. Hwang, and Y. H. Lee, "Effect of size nonuniformities on the bandgap of two dimensional photonic crystals," *Phys. Rev. B*, vol. 59, no. 8, pp. 5463–5469, Feb. 1999.
[14] A. F. Koenderink and W. L. Vos. Optical loss due to intrinsic structural variations of photonic crystals. [Online]. Available: http://arxiv.org/abs/physics/0 406 052
[15] S. G. Johnson, P. Bientsman, M. A. Skorobogatiy, M. Ibanescu, E. Lidorikis, and J. D. Joannopoulos, "Adiabatic theorem and continuous coupled-mode theory for efficient taper transitions in photonic crystals," *Phys. Rev. E*, 2002.
[16] M. L. Povinelli, S. G. Johnson, E. Lidorikis, and J. D. Joannopoulos, "Effect of a photonic bandgap on scattering from waveguide disorder," *Appl. Phys. Lett.*, vol. 84, no. 12, pp. 3639–3639, May 2004.
[17] A. Tafflove and S. Hagness, *Computational Electrodynamics: The Finite Difference Time-Domain Method*. Norwood, MA: Artech House, 2000.
[18] T. Kamalakis, T. Sphicopoulos, and D. Syvridis, "An estimation of performance degradation due to fabrication errors in AWGs," *J. Lightw. Technol.*, vol. 20, no. 9, Sep. 2002.
[19] M. Skorobogatiy, M. Ibanescu, S. G. Johnson, O. Weisberg, T. D. Engeness, M. Soljacic, S. A. Jacobs, and Y. Fink, "Analysis of general geometric scaling perturbations in a transmitting waveguide: Fundamental connection between polarizarion-mode dispersion and group-velocity dispersion," *OSA J. Opt. Soc. Am. B*, vol. 19, no. 12, pp. 2867–2867, Dec. 2002.
[20] Y. Hibino, "Recent advances in high-density and large scale AWG multi/demultiplexers with higher index contrast-based PLCs," *IEEE J. Sel. Topics Quantum Electron.*, vol. 8, no. 6, pp. 1090–1101, Nov. 2022.
[21] H. A. Haus and W. P. Huang, "Mode coupling in tapered structures," *J. Lightw. Technol.*, vol. 7, no. 4, pp. 729–730, Apr. 1989.
[22] J. Jiang, J. Cai, G. P. Nordin, and L. Li, "Parallel microgenetic algorithm design for photonic crystal and waveguide structures," *OSA Opt. Lett.*, vol. 28, no. 23, pp. 2381–2383, Dec. 2003.

[23] C. Manolatou, S. G. Johnson, S. Fan, P. R. Villeneuve, H. A. Haus, and J. D. Joannopoulos, "High density integrated optics," *J. Lightw. Technol.*, vol. 17, no. 9, pp. 1682–1682, Sep. 1999.
[24] M. F. Yanik, H. Altug, J. Vuckovic, and S. Fan, "Sub-micron all-optical digital memory and integration of nano-scale photonic devices without isolators," *J. Lightw. Technol.*, vol. 22, no. 9, pp. 2316–2316, Sep. 2004.
[25] P. Sanchis, P. Bienstman, B. Luyssaert, R. Baets, and J. Marti, "Analysis of Butt coupling in photonic crystals," *IEEE J. Quantum Electron.*, vol. 40, no. 5, pp. 541–550, May 2004.
[26] M. Koshiba, Y. Tsuji, and S. Sasaki, "High-Performance absorbing boundary conditions for photonic crystal waveguide simulations," *IEEE Microw. Compon. Lett.*, vol. 11, no. 4, pp. 152–154, Apr. 2001.

Thomas Kamalakis was born in Athens, Greece, 1975. He received the B.Sc. degree in informatics and the M.Sc. degree in telecommunications (with distinction) from the University of Athens, Athens, Greece, in 1997 and 1999, respectively, where he received the Ph.D. degree in the design and modeling of arrayed waveguide grating devices in 2004.

He is currently a Research Associate for the Optical Communications Laboratory, University of Athens, and an Assistant Lecturer in electronics for the University of Peloponnese, Peloponnese, Greece. He serves as a Consultant for the deployment of optical fibers in the Peloponnese district and participated in the OTEWAVE project of the National Telecommunication Organization of Greece, which dealt with the integration of IP and wavelength division multiplexing (WDM). His research interests include photonic crystal devices and nonlinear effects in optical fibers.

Dr. Kamalakis is a Reviewer for IEEE PHOTONICS TECHNOLOGY LETTERS, IEEE/OSA JOURNAL OF LIGHTWAVE TECHNOLOGY, and IEEE JOURNAL OF QUANTUM ELECTRONICS.

Thomas Sphicopoulos received the B.S. degree in physics from Athens University, Athens, Greece, in 1976, and the D.E.A. and Doctorate degrees in electronics from the University of Paris VI, Paris, France, in 1977 and 1980, respectively, and the Doctorat Es Science from the Ecole Polytechnique Federale de Lausanne, Zurich, Switzerland, in 1986.

From 1976 to 1977, he worked in Thomson CSF Central Research Laboratories, France, on Microwave Oscillators. From 1977 to 1980, he was an Associate Researcher in Thomson CSF Aeronautics Infrastructure Division. In 1980, he joined the Electromagnetism Laboratory, Ecole Polytechnique Federal de Lausanne where he carried out research on applied electromagnetism. Since 1987 he has been with Athens University engaged in research on broad-band communications systems. In 1990, he was elected as an Assistant Professor of Communications in the Department of Informatics and Telecommunications, in 1993 as Associate Professor, and since 1998, he has been a Professor. His main scientific interests are microwave and optical communication systems and networks and techno-economics. He has lead about 40 national and european research and development projects. He has more than 100 publications in scientific journals and conference proceedings. Since 1999, he has been an advisor in several organizations including EETT (Greek NRA for telecommunications) in the fields of market liberalization, spectrum management techniques, and technology convergence.